

Computation of spatial kernel of carbon nanotubes in non-local elasticity theory from helical symmetry lattice dynamics

Veera Sundararaghavan* and Anthony Waas†

Department of Aerospace Engineering

University of Michigan

Ann Arbor, MI 48109, USA.

(Dated: August 21, 2009)

The longitudinal, transverse and torsional wave dispersion curves in single walled carbon nanotube (SWCNT) are used to estimate the non-local kernel for use in continuum elasticity models of nanotubes. The dispersion data for an armchair (10,10) SWCNT was obtained using lattice dynamics of SWNTs while accounting for the helical symmetry of the tubes. In our approach, the Fourier transformed kernel of non-local linear elastic theory is directly estimated by matching the atomistic data to the dispersion curves predicted from non-local beam theory and axisymmetric shell theory. The distribution of kernel weights in the Fourier space indicate that a Gaussian kernel can offer a better prediction for wave dispersion in CNTs than the non-local kernel from gradient theory. Reconstructions of these kernels are provided in this paper and the dispersion data obtained from such kernels are directly compared with gradient theories. The numerically computed kernels obtained from this study will help in development of improved and efficient continuum models for predicting the mechanical response of CNTs.

Keywords: Carbon nanotubes; phonon dispersion; wave propagation; non-local elasticity; shell theory.

I. INTRODUCTION

Non-local continuum field theories are concerned with the physics of material bodies whose behavior at a material point is influenced by the state of all points in the body. For homogeneous and isotropic elastic solids with zero body forces, the non-local theory is expressed by the following equations:

$$s_{ij,i} = \rho \ddot{u}_j, \quad (1)$$

$$s_{ij}(\mathbf{x}) = \int_V \alpha(|\mathbf{x}' - \mathbf{x}|) \sigma_{ij}(\mathbf{x}') dV(\mathbf{x}'), \quad (2)$$

$$\sigma_{ij}(\mathbf{x}') = C_{ijkl} \epsilon_{kl}(\mathbf{x}') \quad (3)$$

$$\epsilon_{ij}(\mathbf{x}') = \frac{1}{2} \left(\frac{\partial u_i(\mathbf{x}')}{\partial x_j'} + \frac{\partial u_j(\mathbf{x}')}{\partial x_i'} \right) \quad (4)$$

where s_{ij} and ϵ_{ij} are stress and strain tensors respectively; C_{ijkl} is the elastic modulus tensor in elasticity theory and u_i is the displacement vector. Non local theory proposed by Eringen¹ assumes that stress (\mathbf{s}) at a point depends on the deformation within a finite zone of influence V by means of a non-local kernel α (a function of Euclidean distance $|\mathbf{x} - \mathbf{x}'|$) that weights the stresses around point \mathbf{x} . The kernel satisfies three important properties: firstly it is maximum at the point of interest and decays around it; secondly, the kernel is normalized with respect to the volume ($\int_V \alpha dV = 1$) and finally, α reverts to a delta function as the zone of influence vanishes which leads to the well known local elasticity formulation. Non-local elasticity theories nominally take into account the multi-atom interactions that determine the stress state at a point. Thus, non-local elasticity may overcome several issues associated with local elasticity, for example, local elasticity predicts infinite stresses at

a crack tip and incorrectly predicts energetics of point defects.

The application of non-local elasticity to nanoscale materials has emerged as an important topic recently. Much attention has been given to the investigation of physical properties of Carbon nanotubes. Nanotubes are expected to be as stiff as graphite along the graphene layers or even reach the stiffness of diamond. This unique mechanical property of the nanotubes combined with their lightness predetermines their usage in composite materials and has motivated computational studies of their elastic behavior. Application of nonlocal theory to study the bending, vibration and buckling behavior of Carbon nanotubes (CNTs)²⁻⁶ has been studied recently within the ‘gradient theory’ which is a form of non-local theory derived for a special class of kernels. Gradient theory can be derived by assuming that the kernel is of a special form (eg. for 2D lattices, $\alpha = (2\pi c^2)^{-1} K_0(\sqrt{\mathbf{x} \cdot \mathbf{x}}/c)$, where K_0 is the modified Bessel function) that satisfies the differential equation: $(1 - c^2 \nabla^2) \alpha = \delta(|\mathbf{x}|)$. The application of this equation to the integral formulation described previously leads to the constitutive relationship in gradient elasticity $(1 - c^2 \nabla^2) \mathbf{s} = \boldsymbol{\sigma}$. The parameter c was explained by Eringen as a product of a material specific parameter (e_0) and an internal characteristic parameter (a). The gradient formulation has been shown to reasonably reproduces the phonon dispersion curve for a Born-Karman model of lattice dynamics (harmonic spring model). However, the ability of such a model to predict complex lattice dynamics such as those obtained in the case of nanotubes is questionable.

Both theoretical analyses and numerical simulations have revealed that wave dispersion relations in the longitudinal and circumferential directions have non-local effects. Wang et al. have studied several vibration prob-

lems of nanotubes based on Flugge elastic shell theory⁷⁻⁹. In a recent study, it was found that the best fit kernel parameter (e_o) changes depending on which atomistically computed vibration modes are fitted to the shell theory (for eg., transverse ($e_o = 0.2$) or torsional ($e_o = 0.4$)). These results present an atomistically validated form of kernel for CNTs; nevertheless the kernel is approximated within the gradient theory and the exact form is not calculated. For a special case of interatomic potentials depending only on pair interactions (or through embedded functions that are function of radial distance only), a direct reconstruction technique for the kernel based on potential description was proposed by Picu¹⁰. However such approaches cannot be used since carbon atom interactions in CNT are typically multibody potentials that depend on atom coordination (Brenner potential) or three or four body interactions (Force field potentials). In this paper, we follow the approach suggested by Eringen to develop the kernel through fitting the predictions of a model kernel with the phonon dispersion curve of the CNT lattice. The Fourier transformed non-local kernel is reproduced for two specific models of nanotube prevalent in literature, the 1D beam model and the axisymmetric shell model based on Flugge theory. The new data from this work indicate that a Gaussian kernel can offer a better prediction for wave dispersion in CNTs than the non-local kernel from gradient theory. Reconstructions of these kernels are provided in this paper and the dispersion data obtained from such kernels are directly compared with gradient theories.

The paper is arranged as follows. In Section II, the essential features of a model of the lattice dynamics of SWNTs based on the explicit accounting for the helical symmetry of the tubes are summarized. The phonon dispersion curves for the nanotube computed from this approach are used to obtain the expression for $\alpha(k)$ (the Fourier transform of the non-local kernel) through comparison with the 1D beam theory and non-local axisymmetric shell theory in Section III and Section IV respectively.

II. ATOMISTIC MODELING OF DISPERSION CURVES OF NANOTUBES

The ideal nanotube structure can be obtained from a graphene sheet by rolling it up along a straight line connecting two lattice points into a seamless cylinder in such a way that the two points coincide. The tube can be specified by the pair of integers (L_1, L_2) that define the lattice translation vector between the two points (coordinate axes ($\mathbf{a}_1, \mathbf{a}_2$) as shown in Fig. 1). The nanotube can be considered as a crystal lattice with a two atoms unit cell and the entire nanotube may be constructed using two screw operators¹¹. A screw operator involves a rotation of the position vector of an atom by an angle ϕ about an axis with rotation matrix \mathbf{S} and a translation of this vector along the same axis. Any cell (\mathbf{l})

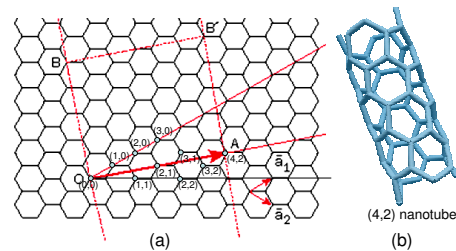


FIG. 1: The nanotube structure is obtained from a graphene sheet by rolling it up along a straight line connecting two lattice points (with translation vector (L_1, L_2)) into a seamless cylinder in such a way that the two points coincide. The figure shows how a unit cell of a (4,2) nanotube (shown in (b)) can be created by rolling the nanotube such that points O and B coincide.

is represented by a combination $\mathbf{l} = (l_1, l_2)$. The effective operators used to obtain the cell are defined as $S(\mathbf{l}) = S_1^{l_1} S_2^{l_2}$ and $\mathbf{t}(\mathbf{l}) = l_1 \mathbf{a}_1 + l_2 \mathbf{a}_2$. Thus, the equilibrium position vector $\mathbf{R}(\mathbf{l}k)$ of the k^{th} atom in the \mathbf{l}^{th} cell is obtained from basis atoms $\mathbf{R}(k) \equiv \mathbf{R}(0k)$ as

$$\mathbf{R}(\mathbf{l}k) = S(\mathbf{l})\mathbf{R}(k) + \mathbf{t}(\mathbf{l}) \quad (5)$$

Each atom is thus uniquely represented by the pair, $\mathbf{l}k$.

A lattice-dynamical model for a SWNT can be developed using the above representation in a similar way to a three-dimensional crystal lattice. This model was originally developed in Popov et. al. (2000)¹². The equation of motion for small displacements $\mathbf{u}(\mathbf{l}k)$ of the atoms from their equilibrium positions are given by

$$m\ddot{\mathbf{u}}_i(\mathbf{l}k) = - \sum_{\mathbf{l}'k'} \Phi_{ij}(\mathbf{l}k, \mathbf{l}'k') u_j(\mathbf{l}'k'), \quad (6)$$

where m is the atomic mass of carbon atom and Φ_{ij} is the force constant matrix (i, j are indices referring to x, y, z directions). The helical symmetry of the tubes necessitates wavelike solutions for the atomic displacement vectors $\mathbf{u}(\mathbf{l}k)$ (in a form similar to Eq. 5) as follows:

$$\mathbf{u}_i(\mathbf{l}k) = \frac{1}{\sqrt{m_k}} \sum_j S_{ij}(\mathbf{l}) e_j(k|\mathbf{q}) \exp\{i[\mathbf{q} \cdot \mathbf{l} - \omega(\mathbf{q})t]\}, \quad (7)$$

with wave vector $\mathbf{q} = (q_1, q_2)$, wave amplitude $e(k|\mathbf{q})$ and angular frequency $\omega(\mathbf{q})$. For carbon nanotubes, in addition to the above equation, rotational boundary condition and translational periodicity constraints of the nanotube are additionally enforced¹² as $q_1 L_1 + q_2 L_2 = 2\pi l$ and $q_1 N_1 + q_2 N_2 = q$. Here, l is an integer number ($l = 0, \dots, N_c - 1$, where N_c is the number of atomic pairs in the translational unit cell of the tube), q is a new, one-dimensional wave vector, and the integers N_1 and N_2 define the primitive translation vector of the tube. The wave-vector components q_1 and q_2 can be expressed

through the parameters q and l and after substituting Eq. 7 in Eq. 6, the equations of motion are obtained in the form:

$$\omega^2(ql)e_i(k|ql) = \sum_{k'j} D_{ij}(kk'|ql)e_j(k'|ql) \quad (8)$$

where D_{ij} is the dynamical matrix. The equations of motion described above yield the eigenvalues $\omega(ql)$ where l labels the modes with a given wave number q ($= ka$, where a is the lattice parameter and $k = \frac{1}{\lambda}$) in the one-dimensional Brillouin zone ($-\pi < q < \pi$).

A force-constant – Valence Force Field (VFF) model¹² of the lattice dynamics was employing nearest neighbor stretch, next-to-nearest-neighbor stretch, in-plane bend, out-of-plane bend and twist interactions was employed to compute the dispersion curves. The calculated phonon dispersion of a armchair (10,10) carbon nanotube in Fig. 2 shows the presence of axisymmetric longitudinal, torsional, and transverse modes at the lowest energies ($\omega < 50\text{cm}^{-1}$). As shown separately in Fig. 2(b), the longitudinal and torsional modes increase linearly with the wave number at large wavelengths and the transverse mode increases as the square of the wave number at large wavelengths. In this work, these axisymmetric modes will be used to identify the non-local kernel of a carbon nanotube. Further, the list of material constants used for subsequent continuum scale analysis of the nanotube (mechanical properties from the force field model, nanotube thickness and bending rigidity taken from literature⁹) are listed in Table 1.

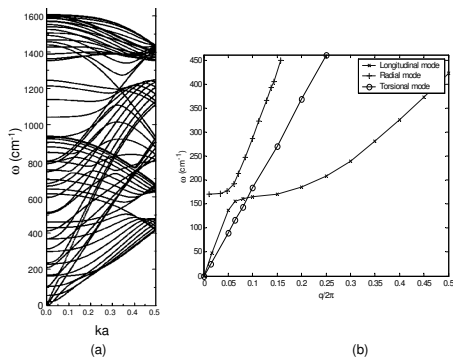


FIG. 2: (a) Atomistically computed dispersion curves for (10,10) single walled carbon nanotube. (b) The axisymmetric modes corresponding to the torsional, transverse and longitudinal vibrations of the SWCNT.

III. COMPARISON WITH 1D NON-LOCAL THEORIES

The classical approach (suggested by Eringen¹) for reconstructing the non-local kernel is to match the dispersion curves of plane waves predicted by the non-local

TABLE I: List of constants for the (10, 10) single walled nanotube

Material constant	Value
Young's modulus E (GPa)	830
Density, ρ (kg/m ³)	2270
Poisson's ratio, ν	0.347
Bending rigidity, D (eV)	1.78
Thickness, h (nm)	0.34
Radius, r (nm)	0.678
C-C distance, a_c (nm)	0.142

theory with atomistically calculated dispersion curves. Dispersion curves of a beam are calculated by using displacement $u(x, t)$ of the plane wave form $u(x, t) = Ue^{i(kx - \omega(k)t)}$, where k is the inverse wavelength, and $\omega(k)$ denotes the frequency of the plane wave in the 1D governing equation $\frac{\partial s}{\partial x} = \rho \frac{\partial^2 u}{\partial t^2}$. For an isotropic linear elastic solid with Youngs modulus (E), Poissons ratio (ν) and density (ρ), this leads to the well-known formula:

$$\frac{\omega}{k} = \sqrt{\frac{E}{\rho}} \sqrt{\alpha(k)} \quad (9)$$

where $\alpha(k)$ represents the Fourier transform of α (defined as $\alpha(k) = \int_{-\infty}^{\infty} \alpha(|x|)e^{-ikx} dx$).

Gradient theory can be derived by assuming that the kernel is of a special form that satisfies the differential equation:

$$(1 - c^2 \nabla^2) \alpha = \delta(|x|) \quad (10)$$

Substitution of the above relation in Eq. 2 results in the following constitutive equation:

$$\sigma = (1 - c^2 \nabla^2) s \quad (11)$$

As shown in Eringen, Fourier transform of the kernel can be approximated (for $k^2 a^2 \ll 1$) as:

$$\alpha(k) = \frac{2}{k^2 a^2} (1 - \cos(ka)) \approx (1 + e_o^2 a^2 k^2)^{-1} \quad (12)$$

It can be verified that this approximation indeed satisfies the above-mentioned differential equation (Eq. 10). Eringen demonstrated that such a kernel will be able to approximate the dispersion curve of a Born Karman model ($\frac{\omega a}{c_o} = 2 \sin(ka/2)$) of lattice dynamics (harmonic spring model with nearest neighbor interactions) if $e_o = 0.39$ (see Fig. 3). In Eringen's work, fitting is performed such that the frequency predicted by the non-local elasticity model at the end of the Brillouin zone (at $ka = \pi$) is same as the atomistic model. Alternate approaches suggested for computing the non-local parameter (e_o) in gradient theory include matching atomistic computations with theoretical predictions of continuum quantities such as elastic modulus¹³ and buckling strain⁶. Zhang et al.⁶ estimated $e_o = 0.82$ by matching

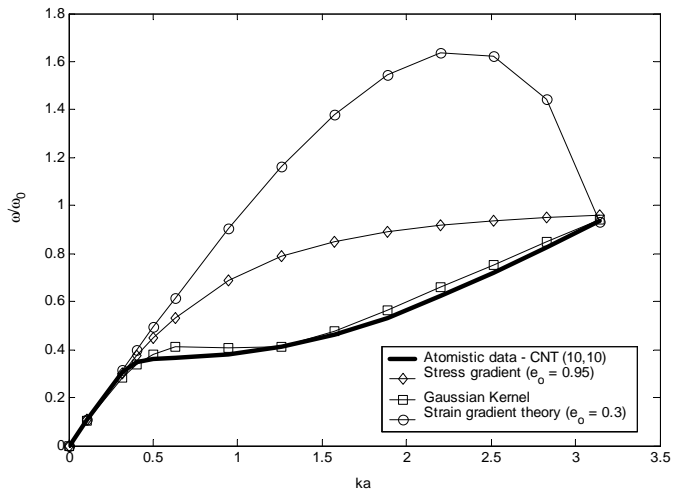


FIG. 3: Phonon dispersion curve (comparison with the atomistically computed longitudinal mode of (10,10) nanotube) with (i) Stress gradient theory (ii) Strain gradient theory (iii) Gaussian kernel.

the theoretical buckling strain obtained by the nonlocal thin shell model to those from molecular mechanics simulations given by Sears and Batra¹⁴. From our study, as shown in Fig. 3, we find that $e_0 = 0.95$ best matches the longitudinal mode dispersion observed from the atomistic data. However, the group and phase velocities at other wavelengths do not match well with atomistic predictions. In order to better fit the atomistic data, we fitted the kernel ($\alpha(k)$) from atomistic data using Eq. 9. The Fourier transformed kernel from atomistic data is plotted against that of stress gradient model ($e_0 = 0.95$) in Fig. 4. Through inspection of the atomistic data in Fig. 4, it can be seen that the reconstructed $\alpha(k)$ closely represents a kernel of Gaussian-type. The Fourier transform of the kernel from atomistic data is well represented by the following function:

$$\alpha(k) = 0.09 + 0.91 \exp(-(ka)^2/0.4) \quad (13)$$

In order to understand the variation of α in real space, we reconstructed the kernel weights using an inverse Fourier transform (using $a = 0.213$ nm) and the result is plotted in Fig. 5. The results reveal that the kernel is non-zero up to a distance of 1.3 nm from the point under consideration. The Gaussian kernel (inverse Fourier transform) of the above function is given below (where $y = |\mathbf{x}' - \mathbf{x}|$ is in Angstrom units, and $\delta(\cdot)$ is the delta function.):

$$\alpha(y) = 0.09\delta(y) + 0.076 \exp(-(y/6.736)^2) \quad (14)$$

Remark: Another theory, namely, the strain gradient approach, has been previously used for computing the response of nanotubes. In strain gradient theory, the 1D

constitutive relationship can be expressed in the form:

$$s = E(\epsilon + (e_0 a)^2 \frac{\partial^2 \epsilon}{\partial x^2}) \quad (15)$$

Comparison of the dispersion curve predicted by this model ($\frac{\omega}{k} = \sqrt{\frac{E}{\rho} \sqrt{1 - (e_0 a)^2 k^2}}$) with the atomistic dispersion curves leads to $e_0 = 0.304$. This favorably compares with the prediction of Wang and Hu¹⁵ who proposed $e_0 = 0.288$ within the strain gradient approach by comparing with molecular dynamics simulations. The theory is, in fact, a second order truncation of the series represented by the gradient model³ and as seen in Fig. 3 does not provide a good fit to the atomistic dispersion curves.

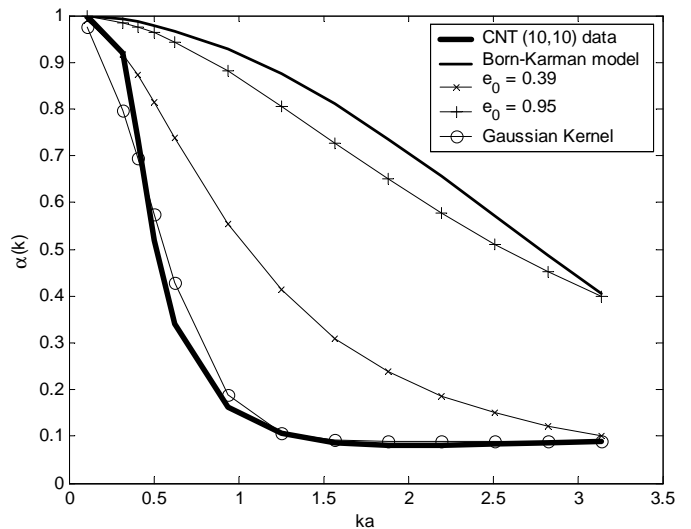


FIG. 4: The Fourier transform of the kernel computed using atomistic data and Eq. 9 is plotted against Fourier transformed kernel of (i) Stress gradient model (ii) Gaussian Kernel model. The Born-Karman model and its stress gradient theory fit as obtained by Eringen¹ is also indicated.

IV. COMPUTATION OF NON-LOCAL KERNEL USING FLUGGE THEORY

When the radial and/or circumferential displacements dominate in the wave motion, CNTs should only be modeled as elastic shell rather than elastic beam models in the continuum modeling theory. To establish CNT wave propagation analysis with the nonlocal elastic shell theory, a polar coordinate system is taken with x and θ denoting the longitudinal and angular circumferential coordinates. In the nonlocal elastic shell theory, the local stress and moment resultants are defined by referencing the kinematic relations in Flugge's shell theory¹⁶ for axisymmetric deformation ($\frac{\partial}{\partial \theta}(\cdot) = 0$):

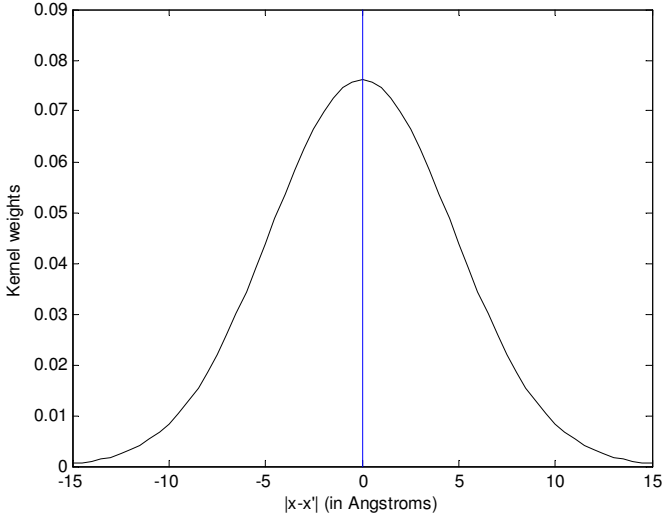


FIG. 5: The best kernel for the 1D approximation of a nanotube (as reconstructed from atomistic data).

$$N_x^l = \frac{Eh}{r(1-\nu^2)} \left(-\nu w + r \frac{du}{dx} \right) + \frac{D}{r} \frac{d^2w}{dx^2} \quad (16)$$

$$N_\theta^l = \frac{Eh}{r(1-\nu^2)} \left(-w + r\nu \frac{du}{dx} \right) - \frac{D}{r^3} w \quad (17)$$

$$N_{x\theta}^l = \frac{Eh}{2r(1+\nu)} r \frac{dv}{dx} - \frac{D}{r^2} \frac{1-\nu}{2} \frac{dv}{dx} \quad (18)$$

$$M_x^l = -\frac{D}{r^2} \left(r^2 \frac{d^2w}{dx^2} + r \frac{du}{dx} \right) \quad (19)$$

$$M_{x\theta}^l = -\frac{D}{r} (1-\nu) \frac{dv}{dx} \quad (20)$$

where $D = \frac{Eh^3}{1-\nu^2}$ is bending rigidity in shell theory, r and h are the thickness and radius of the nanotube shell respectively. u , v and w are displacement variables in axial, radial and circumferential directions of the nanotube. The local values of the forces and moments can be used within the non-local theory to compute the kernel-averaged forces and moments. Consistent with the assumption of axisymmetric deformation, an axisymmetric kernel is utilized to describe these non-local counterparts:

$$\Gamma(\mathbf{x}) = \int_V \alpha(|\mathbf{x} - \mathbf{x}'|) \Gamma^l(\mathbf{x}') dx' \quad (21)$$

The dynamic equilibrium equations of the stress and moment resultants are given as¹⁶:

$$r \frac{\partial N_x}{\partial x} - \rho hr \frac{\partial^2 u}{\partial t^2} = 0 \quad (22)$$

$$r^2 \frac{\partial N_{x\theta}}{\partial x} - r \frac{\partial M_{x\theta}}{\partial x} - \rho hr^2 \frac{\partial^2 v}{\partial t^2} = 0 \quad (23)$$

$$r^2 \frac{\partial^2 M_x}{\partial x^2} + r N_\theta - \rho hr^2 \frac{\partial^2 w}{\partial t^2} = 0 \quad (24)$$

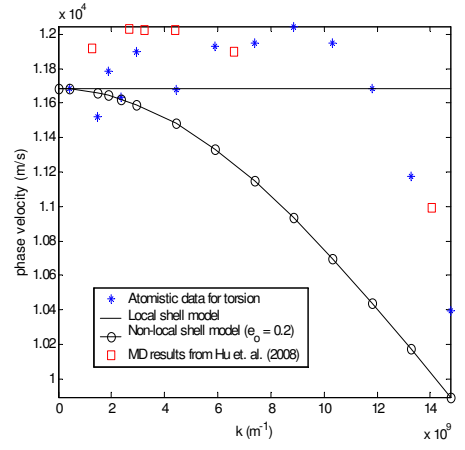


FIG. 6: Dispersion relation of torsional wave in the armchair (10,10) single walled nanotube. The atomistic data is compared with published molecular dynamics data⁹. The curve predicted by the local shell model ($e_o = 0$) and the nonlocal shell model ($e_o = 0.2$) are indicated.

Eq. 23 represents the purely torsional motion of the shell. The plane waves representing displacements in the radial, transverse and circumferential directions are assumed to be independent of θ due to axisymmetry. Substituting the expression $v(x, t) = V e^{i(kx - \omega t)}$ to Eq. 23 leads to the dispersion relation of torsion wave:

$$\frac{\omega}{k} = \sqrt{\frac{E}{2\rho(1+\nu)} + \frac{3}{2} \frac{D(1-\nu)}{\rho hr^2} \sqrt{\alpha(k)}} \quad (25)$$

Dispersion relation of torsional wave (in terms of phase velocity) in the armchair (10,10) single walled nanotube is shown in Fig 6. The atomistic data is compared with published molecular dynamics data⁹ as well as those predicted the local shell model ($e_o = 0$) and the nonlocal shell model ($e_o = 0.2$).

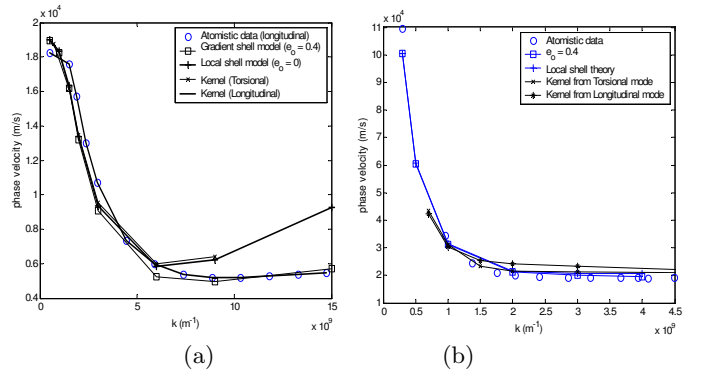


FIG. 7: Dispersion relation of (a) longitudinal wave and (b) transverse wave in the armchair (10,10) single walled nanotube. The curve predicted by the local shell model ($e_o = 0$) and the nonlocal shell model ($e_o = 0.4$) are indicated. The curve predicted by the kernel reconstructed from torsional mode data and the longitudinal mode data are also indicated.

Substitution of the displacements $u(x, t) = Ue^{i(kx - \omega t)}$ and $w(x, t) = We^{i(kx - \omega t)}$ in Eq. 22 and Eq. 24 lead to the dispersion relation of longitudinal and radial waves. The dispersion relation is directly expressed in terms of the unknown non-local kernel in both cases. Fourier transform of the non-local kernel ($\alpha(k)$) can be reconstructed by plugging in the dispersion data (ω versus k) obtained from atomistic simulations directly in the following expression (where $|\cdot|$ is the matrix determinant):

$$\begin{vmatrix} -\frac{\nu Eh}{r(1-\nu^2)} - \frac{Dk^2}{r} & \frac{ikEh}{1-\nu^2} - \frac{i\rho h\omega^2}{k\alpha(k)} \\ r^2k^2D + \frac{Eh}{k^2(1-\nu^2)} + \frac{D}{r^2k^2} - \frac{\rho hr^2\omega^2}{k^2\alpha(k)} & -ikrD - \frac{iEhr\nu}{k(1-\nu^2)} \end{vmatrix} = 0 \quad (26)$$

Dispersion relation of torsional and longitudinal wave (in terms of phase velocity) in the armchair (10,10) single walled nanotube computed from atomistic data is shown in Fig. 6. The atomistic data is compared with the curve predicted by the local shell model ($e_o = 0$) and the nonlocal shell model ($e_o = 0.4$). In order to reconstruct the true (axisymmetric) kernel that results in the atomistically calculated dispersion curve, the Fourier transform ($\alpha(k)$) is reconstructed directly from atomistic data based on Eqs. 25–26. The results are plotted against the kernel of the stress gradient model in Fig. 8. It is seen that the gradient model involves a monotonously decreasing kernel whereas the atomistic data predicts non-monotonous kernels with Gaussian nature. In addition, it is seen that the best-fit parameter (e_o) in gradient theory is different in the case of torsional ($e_o = 0.2$) and longitudinal modes ($e_o = 0.4$). Similar values were predicted in Hu et al⁹ by comparing molecular dynamics simulation data with shell theory. From the results in Fig. 8, it is evident that gradient theory, with its inherent approximations, cannot fully describe the dynamics of the single walled nanotube. The best fit non-local kernel is estimated by directly fitting the atomistic data in Fig. 8.

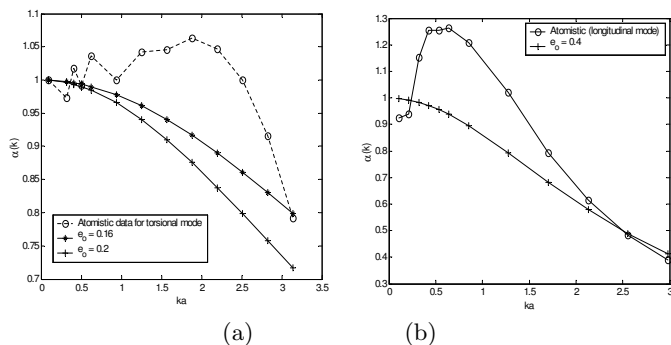


FIG. 8: The Fourier transform of the kernel computed using atomistic data and Eqs. 25–26 is plotted against the kernel of the stress gradient model for (a) Torsional mode and (b) Longitudinal mode.

In Fig. 9(a), we have plotted the best fit Gaussian-type kernel obtained from atomistic data of the longitudinal mode. The Fourier transform of the kernel obtained from atomistic data is given by the following function:

$$\alpha(k) = 0.343 + 1.03 \exp(-(ka)^2/3.6) - 0.373 \exp(-(ka)^2/0.12) \quad (27)$$

The real space reconstruction of the kernel is shown in Fig. 9(b) as a function of distance from the point of interest.

In contrast to our predictions from the 1D model (Fig. 5), it is seen that kernel weights become negative at larger distances. These effects have been previously seen in the kernels reconstructed by Picu¹⁰ for metallic systems. The improvement in the prediction of dispersion curves when using a Gaussian model is illustrated by comparing the reconstructed dispersion curves from the local shell model ($e_o = 0$, gradient shell model ($e_o = 0.4$) and the Gaussian kernel-based shell model with the atomistic dispersion curves of a (10,10) nanotube in Fig. 10. The best fit Gaussian kernel (in real space) is as follows (where $y = |\mathbf{x}' - \mathbf{x}|$ is in Angstrom units)::

$$\alpha(y) = 0.343\delta(y) + 0.259 \exp(-(y/2.245)^2) - 0.017 \exp(-(y/12.298)^2) \quad (28)$$

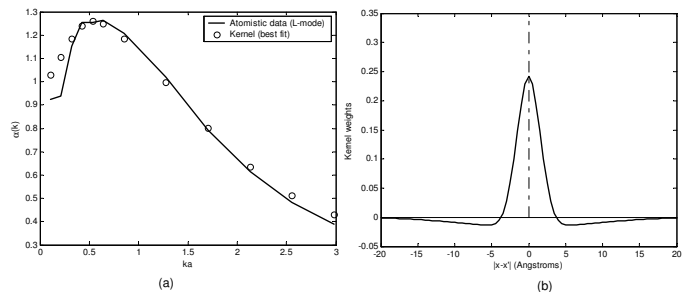


FIG. 9: The best fit kernel obtained from atomistic data of the longitudinal mode (left) the Fourier transformed kernel (right) Reconstructed kernel weights plotted as a function of distance from the point of interest. Kernel weights become negative at larger distances (also Ref. Picu¹⁰).

V. CONCLUSIONS

The longitudinal, transverse and torsional axisymmetric mode wave dispersions in single walled carbon nanotube (SWCNT) were studied in the context of nonlocal elasticity theory. The dispersion data for an armchair (10,10) SWCNT was obtained from lattice dynamics of SWNTs while accounting for the helical symmetry of the tubes. The data was then used to predict the

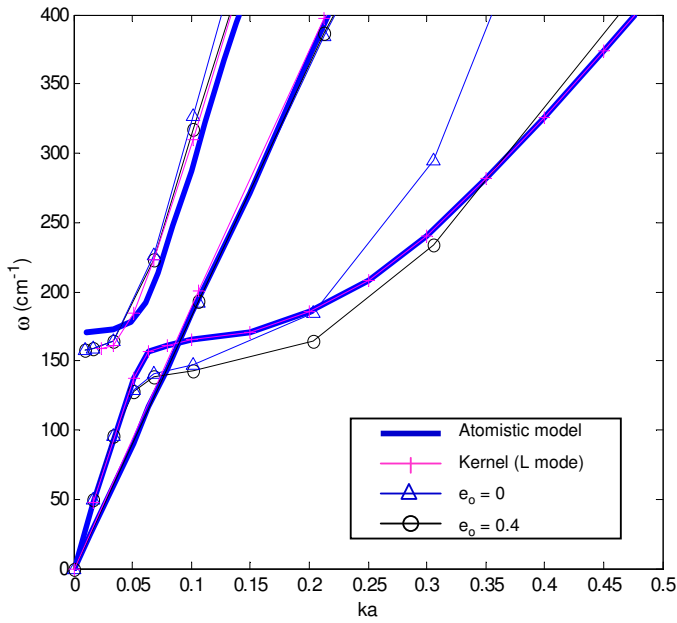


FIG. 10: The reconstructed dispersion curves from the local shell model ($e_o = 0$), gradient shell model ($e_o = 0.4$) and the Gaussian kernel-based shell model are superposed with atomistic dispersion curves of a (10,10) nanotube. Only the low-energy modes are shown.

material parameter (e_o) in gradient theory for 1D beam and axisymmetric cylindrical shell model of a nanotube. The prediction was made using the approach of Eringen¹ by matching the frequency predicted by the non-local elasticity model at the end of the Brillouin zone to the atomistic model. It is seen that stress and strain gradient model incur significant errors in both the phase and group velocity when compared to the atomistic model. To improve upon the gradient models, we estimated the Fourier transformed kernel of non-local linear elastic theory by directly matching the atomistic data to the dispersion curves predicted from generalized non-local beam theory and shell theory. The results of this new study indicate that a Gaussian kernel is able to offer a better prediction for transverse and torsional wave dispersion in CNTs than the non-local kernel from gradient theory. Reconstructions of these kernels are provided in this paper and the data is compared directly with stress gradient theory. The results will help in development of improved and efficient continuum models for predicting the mechanical response of CNTs.

* Electronic address: vs85@cornell.edu, Assistant--Professor--Corresponding--author

† Electronic address: dcw@umich.edu, Professor

- [1] A.C. Eringen, On differential equations of nonlocal elasticity and solutions of screw dislocation and surface waves, *J. Appl. Phys.* 54 (1983), p. 4703–4710.
- [2] J. Peddieson, G.R. Buchanan and R.P. McNitt, Application of nonlocal continuum models to nanotechnology, *Int. J. Eng. Sci.* 41 (2003), pp. 305312.
- [3] D. Kumar, C. Heinrich, and A. M. Waas, Buckling analysis of carbon nanotubes modeled using nonlocal continuum theories, *J. Appl. Phys.* 103 (2008), p. 073521.
- [4] L.J. Sudak, Column buckling of multiwalled carbon nanotubes using nonlocal continuum mechanics, *J. Appl. Phys.* 94 (11) (2003), p. 7281.
- [5] C.T. Sun and H. Zhang, Size-dependent elastic moduli of platelike nanomaterials, *J. Appl. Phys.* 93 (2003), pp. 12121218.
- [6] Y.Q. Zhang, G.R. Liu and X.Y. Xie, Free transverse vibration of double-walled carbon nanotubes using a theory of nonlocal elasticity, *Phys. Rev. B* 71 (2005), p. 195404.
- [7] Q. Wang, V. K. Varadan, Application of nonlocal elastic shell theory in wave propagation analysis of carbon nanotubes, *Smart Mater. Struct.* 16 (2007), pp. 178190.
- [8] C. Y. Wang, C. Q. Ru, and A. Mioduchowski, Axisymmetric and beamlike vibrations of multiwall carbon nanotubes, *Physical Review B* 72 (2005), pp. 075414(1-10).
- [9] Yan-Gao Hu, K.M. Liew, Q. Wang, X.Q. He, B.I. Yakobson, Nonlocal shell model for elastic wave propagation in single- and double-walled carbon nanotubes, *Journal of the Mechanics and Physics of Solids*, 56(12) (2008), pp. 3475-3485.
- [10] R.C. Picu, On the functional form of non-local elasticity kernels, *Journal of the Mechanics and Physics of Solids*, 50(9) (2002), pp. 1923-1939.
- [11] C.T. White, D.H. Robertson, and J.W. Mintmire, Helical and rotational symmetries of nanoscale graphitic tubules, *Phys. Rev. B*, 47 (1993), p. 5485.
- [12] V.N. Popov, V.E. Van Doren, Elastic properties of single-walled nanotubes, *Physical Rev B*, 61(4) (2000), p. 3078–3084.
- [13] Q. Wang, Q. K. Han, B. C. Wen, Estimate of material property of carbon nanotubes via nonlocal elasticity, *Adv. Theor. Appl. Mech.* (online), 1(1-4) (2008), pp. 1-10.
- [14] A. Sears and R.C. Batra, Macroscopic properties of carbon nanotubes from molecularmechanics simulations, *Phys. Rev. B* 69 (2004), p. 235406.
- [15] L.F. Wang, H.Y. Hu, Flexural wave propagation in single-walled carbon nanotubes, *Physical Review B*, 71 (2005), 195412.
- [16] W. Flugge, *Stresses in Shells*, Springer, Berlin/Heidelberg (1960).